Accepted Manuscript

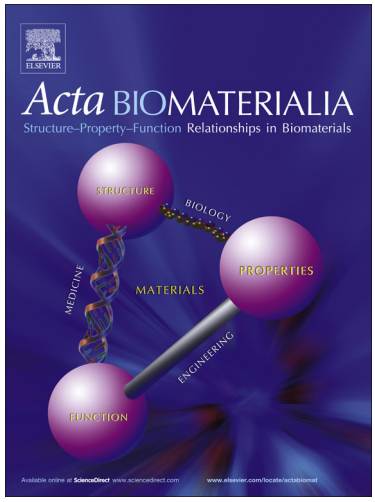

Release of bioactive peptides from polyurethane films *in vitro* and *in vivo*: Effect of polymer composition

Jing Zhang, Trent M. Woodruff, Richard J. Clark, Darren J. Martin, Rodney F. Minchin

PII: S1742-7061(16)30252-5
DOI: http://dx.doi.org/10.1016/j.actbio.2016.05.034
Reference: ACTBIO 4266

To appear in: *Acta Biomaterialia*

Received Date: 11 January 2016
Revised Date: 26 April 2016
Accepted Date: 3 May 2016

Please cite this article as: Zhang, J., Woodruff, T.M., Clark, R.J., Martin, D.J., Minchin, R.F., Release of bioactive peptides from polyurethane films *in vitro* and *in vivo*: Effect of polymer composition, *Acta Biomaterialia* (2016), doi: http://dx.doi.org/10.1016/j.actbio.2016.05.034

Release of bioactive peptides from polyurethane films *in vitro* and *in vivo*: Effect of polymer composition.

Jing Zhang[a], Trent M. Woodruff[a], Richard J. Clark[a], Darren J. Martin[b], Rodney F. Minchin[a*]

[a] *School of Biomedical Sciences, University of Queensland, St Lucia, Queensland, 4072, Australia*

[b] *Australian Institute for Bioengineering and Nanotechnology, University of Queensland, St Lucia, Queensland, 4072, Australia*

*Corresponding author:

School of Biomedical Sciences,

University of Queensland,

St Lucia, Queensland, 4072, Australia

Telephone 61-7-3346-1620

Fax: 61-7-3365-1766

Email: r.minchin@uq.edu.au

Abstract

Thermoplastic polyurethanes (TPUs) are widely used in biomedical applications due to their excellent biocompatibility. Their role as matrices for the delivery of small molecule therapeutics has been widely reported. However, very little is known about the release of bioactive peptides from this class of polymers. Here, we report the release of linear and cyclic peptides from TPUs with different hard and soft segments. Solvent casting of the TPU at room temperature mixed with the different peptides resulted in reproducible efflux profiles with no evidence of drug degradation. Peptide release was dependent on the size as well as the composition of the TPU. Tecoflex 80A (T80A) showed more extensive release than ElastEon 5-325, which correlated with a degree of hydration. It was also shown that the composition of the medium influenced the rate and extent of peptide efflux. Blending the different TPUs allowed for better control of peptide efflux, especially the initial burst effect. Peptide-loaded TPU prolonged the plasma levels of the anti-inflammatory cyclic peptide PMX53, which normally has a plasma half-life of less than 30 min. Using a blend of T80A and E5-325, therapeutic plasma levels of PMX53 were observed up to 9 days following a single intraperitoneal implantation of the drug-loaded film. PMX53 released from the blended TPUs significantly inhibited B16-F10 melanoma tumor growth in mice demonstrating its bioactivity *in vivo*. This study provides important findings for TPU-based therapeutic peptide delivery that could improve the pharmacological utility of peptides as therapeutics.

Keywords: polyurethane, drug release, peptide, anti-inflammatory

1. Introduction

Bioactive peptides are amongst the fastest growing class of therapeutics under development for the treatment of human disease. They can be highly specific and potent in their pharmacological effects, but suffer from limited modes of delivery, poor bioavailability and rapid clearance [1]. Not surprisingly, considerable effort has been made to formulate peptide-based drugs that enhance their availability or increase their biological stability [2]. This has led to a rapd growth in recent approvals of peptides as therapeutics [3]. One approach to overcome some of the limitations of peptides is to deliver them within a matrix that prevents their rapid clearance in the body and provides prolonged release over days or even months. Because of their high potency, peptides may be attractive candidates for sustained release formulations since much less drug is required compared to many small molecule therapeutics.

Thermoplastic polyurethanes (TPUs) are widely used for implantable devices because of their excellent mechanical properties and biocompatibility [4, 5]. They also have proven versatility for the delivery of therapeutics such as antimicrobial agents, anticancer drugs and anti-inflammatory drugs [6-10]. TPUs can be synthesized from a wide variety of precursors for a range of biological applications. They comprise a mixture of hard and soft segments that are thermodynamically incompatible forming micro-domains as a result of polymerization-induced phase separation [11, 12]. At ambient temperature, the high polarity of the hard segments creates non-covalent cross linking and cohesion between the polymer chains while the long soft segments impart flexibility. The micro-domains preferentially interact with different small molecule drugs depending on their physicochemical properties. Consequently,

as drug delivery matrices, TPUs can be formulated differently to suit the characteristics of the drug.

Biodegradable TPU scaffolds can produce prolonged delivery of large proteins such as insulin-like growth factor [13], bone morphogenic protein-2 [14, 15] and platelet-derived growth factor [16]. However, there are very few studies on the release of peptides from different polyurethanes. Li *et al* reported the controlled release of insulin from biodegradable poly(ether-urethane) hydrogels over 10 days [17] while Wang *et al* recently showed that the peptide Bmap-28 could be released from the hydrophilic polyurethane PEGU25 over more than 20 days [18]. Both approaches used a biodegradable matrix for delivery and therefore were designed as stand-alone delivery systems. By contrast, non-degradable TPUs are widely used in medical devices and implants because they are soft and flexible but highly durable. This has been exploited for drug delivery by impregnating polyurethane-based implants such as catheters, coatings and dressings with different therapeutics [19-21]. A major advantage of using non-biodegradable TPU's for drug delivery is their common use in components of implantable devices. Moreover, the biomedical TPUs are easily to cast and have high drug uptake capacity. However, there are few studies into the release of bioactive peptides from non-biodegradable TPUs or whether these polymers have any advantages as reservoirs for prolonged delivery of peptides *in vivo*.

The goal of the current study was to investigate the release of peptides from medical-grade non-biodegradable TPUs used with implantable devices. Several peptides developed for the treatment of inflammatory diseases were compared with a number of other linear and cyclic peptides to better understand how release of these molecules from the TPUs could be controlled. TPUs with different soft and hard segments were studied and the results demonstrate the flexibility of TPUs for controlled peptide release both *in vitro* and *in vivo*.

The novel approaches reported here have broad application and may improve the pharmacological utility of many peptides as therapeutics.

2. Materials and methods

2.1 Materials

The polyurethanes ElastEon (E5-325) and Tecoflex 80A (T80A) were kindly supplied by AorTech Biomaterials Pty Ltd. PMX53 and SFTI-1 were synthesized as previously described [22, 23]. Xen2174 was a generous gift from Prof Richard Lewis (University of Queensland). All other peptides were synthesised by solid phase peptide synthesis with 9*H*-fluoren-9-ylmethoxycarbonyl (Fmoc) chemistry on either 2-Cl-trityl chloride or Rink-Amide-MBHA resin using previously described procedures [24]. Resins, Fmoc-L-amino acids and reagents were obtained from Iris Biotech GmbH (Marktredwitz, Germany). The peptides were cleaved from resin using TFA with triisopropylsilane (TIPS) and H_2O as scavengers (9.5:2.5:2.5 TFA:TIPS:H_2O) at room temperature for 2 hr. TFA was dried down to 1 ml with nitrogen, and the peptide was precipitated in ice-cold ether, filtered and dissolved in 50% CH_3CN containing 0.05% TFA, then lyophilized. The crude peptides were purified by RP-HPLC on a C_{18} column using a gradient of 0–80% B (Buffer A: H_2O/0.05% TFA; Buffer B: 90% CH_3CN/10% H_2O/0.045% TFA) over 80 min. ESI-MS was used to confirm the molecular mass of the synthesized peptide. All other chemicals were of analytical grade.

2.2 Measurement of peptides by liquid chromatography-mass spectrometry (LC-MS)

Peptides were analyzed by LC-MS using an Agilent API 3200 LC/MS/MS. Samples (5 µl) were injected onto an Agilent C18 column 2.1 x 150 mm and eluted using a water-acetonitrile gradient: 5% acetonitrile containing 0.1% formic acid linear increase to 100%

from 0 to 0.2 min, hold at 100% acetonitrile/0.1% formic acid from 0.2 to 5 min, and linear decrease to 5% acetonitrile/0.1% formic acid from 5.0 to 5.1 min, hold at 5% acetonitrile/0.1% formic acid for 20 mins, at the flow rate of 150 µl/min. The column temperature was 40°C and the sample plate temperature was 4°C. The different peptides were monitored at specific ions determined during assay validation experiments. A standard curve for each peptide was constructed using the same extraction procedure as the samples.

2.3 Preparation of peptide-loaded polyurethane films

Each TPU was dried at 60°C for 1 day prior to use. They were then dissolved in dichloromethane at a concentration of 5% (wt/v). When peptides were co-solvent cast, they were dissolved in methanol and mixed with the TPUs solution. The mixed solution was poured into a Teflon dish and dried at room temperature for 3 hr in a stream of nitrogen gas. Films were then annealed under vacuum at room temperature until the weight reached equilibrium. Under these conditions, each of the peptides examined were stable, whereas heating to 60°C or using alternative solvents led to peptide degradation (data not shown). Films were typically 1-2 mm in thickness [25].

2.4 In vitro release of peptides from polyurethane films

Peptide-loaded films were cut into 1 cm^2, immersed in 4.5 ml medium (Milli Q water, PBS or 10% FBS in RPMI) with constant mixing on a rotating wheel at 37°C. Samples (0.4 ml) were withdrawn at each time point and freeze-dried. For the release of peptide in RPMI with 10% FBS, acetonitrile containing 1% formic acid were added into each samples (3:1 v/v) to precipitate proteins and samples were centrifuged at 13000 g for 10 min. Supernatant (1.4 ml) was withdrawn and freeze-dried. All samples were re-dissolved in 50 µl methanol

and centrifuged at 13000 g for 1 min to remove undissolved salts. Supernatant (5 µl) was analyzed by LC-MS as described above.

2.5 Bioactivity of released peptide

To measure the bioactivity of the peptide released from the TPU films, U937 cells, grown in RPMI 1640 medium with 10% FBS, 2 mM glutamine and penicillin (50 U/ml)/streptomycin (50 µg/ml) at 37^{o}C with 5% CO_2, were differentiated with 1 mM N6-2'-O-dibutyryladenosine 3':5'-cyclic monophosphate for 48 h to increase cell surface expression of C5aR. Differentiated cells were centrifuged at 400 g for 5 min to remove the growth medium and resuspended in Fluo-4 NW dye solution (Invitrogen). Cells (125,000 cells per well) were plated in 96-well plates coated with polylysine in Fluo-4-NW dye solution, incubated for 30 min at 37^{o}C and then centrifuged 400 g for 3 min. PMX53 (0.1 µM or 1 µM), or solution containing released peptides, was added to each well. After 10 min, recombinant human C5a (10 nM) were added to each well and intracellular Ca^{2+} concentration was measured by recording fluorescence at an excitation wavelength of 495 nm and an emission wavelength of 516 nm. To examine the activity of the released PMX53, 0.4 ml samples were collected after 72 hr.

2.6 In vivo pharmacokinetic studies

All animal experiments were performed in accordance with approval from the University of Queensland Animal Ethics Committee, Australia. Male C57BL/6 mice of 6 to 8 weeks old were housed in cages and given free access to standard food and water, and acclimated two days prior to surgery. The animals were anesthetized with 5% isoflurane in 100% oxygen and then maintained using 1 to 2% isoflurane in 100% oxygen. A small incision was made in the

abdomen and polyurethane films containing 200 µg of PMX53 were implanted. The incision was sutured and cleaned. The animals were allowed to recover from anaesthesia. This site was chosen for implantation because of the simplicity of the surgery (rapid recovery by the animals) and the practicalities of implanting a disc of ~ 5 mm diameter. It was also observed that absorption of PMX53 from the abdomen was rapid and complete (see Fig 6A).

Blood samples were collected at each time point into heparinized tubes by cardiac puncture. The blood samples were immediately centrifuged at 13000 g for 1 min at room temperature. The plasma samples were collected. JPE1375 was added into each time point sample as an internal standard just prior to the addition of acetonitrile containing 1% formic acid (3:1 v/v) to precipitate proteins. Samples were centrifuged at 13000 g for 10 min. Supernatant was recovered and freeze-dried. All samples were re-dissolved in 50 µl methanol and centrifuged at 13000 g for 1 min to remove undissolved salts. Supernatant (5 µl) was injected into the LC-MS. A standard curve were prepared in plasma and processed using the same method.

At each time point when the animals were sacrificed, the implanted films were collected and briefly rinsed in H_2O. Films were dried using filter paper before immersing in 1 ml ethanol for 24 hr. The amount of PMX53 in the methanol was measured using LC-MS. The amount of PMX53 released from films was calculated as the total amount PMX53 casted with each film minus the amount remaining in the film at the end of the experiment.

2.7 In vivo pharmacodynamic studies

To examine whether PMX53 released from TPU films retain its bioactivity, the effect of released PMX53 on B16-F10 melanoma tumor growth as evaluated. B16-F10 cells (ATCC, mouse melanoma) were cultured *in vitro* in DMEM medium containing 10% FBS, 2 mM glutamine, and penicillin (50 U/ml) /streptomycin (50 µg/ml) at 37^{o}C with 5% CO_2. When

the cells approached 80-90% confluent, cells were trypsinised and resuspended in PBS. Each C57BL/6 mouse was injected with B16-F10 melanoma cells (200,000 in 100ul) subcutaneously in the rear right flank. Body weight was monitored daily. On the fourth day after cells injection, mice were anaesthetised and implanted with a blended T80A:E5-325 (1:1) film with or without 200 µg of PMX53, as described above. Six days after injection of cells, mice were anesthetized and their tumors were measured with callipers every day until the tumor size reached 800 mm^3, following which the animals were sacrificed. Tumor volume was calculated using the following formula:

$$\text{Volume} = \frac{\text{length} \times \text{width}^2}{2}$$

2.8 Statistical analysis

In vitro and *in vivo* drug release and tumor volume data were analyzed by ANOVA using Prism Software GraphPad. *In vivo* plasma levels of PMX53 were modelled by nonlinear least-squares regression (Prism Software, GraphPad) using various equations (see Results). Stability of peptides and Ca^{2+} measurement data were analyzed using the Student's t-test. All experiments were conducted at least in triplicate. Data are presented as mean ± s.e.m.

3. Results

3.1 In vitro release of peptides from TPUs

A number of different linear and cyclic peptides (Table 1) were studied for release from two different biomedical grade TPUs, which differ in their hard and soft segment composition [25]. Tecoflex 80A (T80A) has a poly(tetramethylene oxide) soft segment and

an aliphatic 4,4'-methylenebis (cyclohexyl) (H_{12}MDI) hard segment, while ElastEon 5325 (E5-325) has a 4,4-methylenediphenyl hard segment and a mixed macrodiol of α,ω-hydroxy-terminated poly-dimethylsiloxane and polyhexamethylene oxide soft segment. T80A has been used in cardiovascular applications [26], vascular grafts [27] and stent production [28] while E5-325 and its analogs have been employed in arthroplasty devices [29], pacing lead insulation and heart valves [30]. These different hard and soft segments produce polymer composites with different physical properties [25] and hemocompatabilities [31]. The peptides chosen for this study ranged in molecular weights from 830 to 1500 daltons and target several different receptors *in vivo* (Table 1).

Typical release profiles for each of the peptides from T80A are shown in Fig. 1. There was considerable variation between the rate and extent of release for the different peptides, although all reached equilibrium by 48 hr. The smaller molecules (PMX53, PXM201 and PMX205 [32]) showed similar release profiles reaching more than 70% by 72 hr. By contrast, the larger peptides (SFT-1 and Xen2174) showed very little release over this time. For the linear peptide (JPE1375 [33]), approximately 30% of the drug was released over 72 hr.

Efflux of the different peptides from T80A and E5-325 with respect to molecular size is shown in Fig 2. For T80A, there was a significant correlation between cumulative release over 72 h and molecular weight ($R^2 = 0.911$, $p < 0.05$). This is in agreement with the very rapid release of the small molecule drug rhodamine (Mol wt 479)) reported previously [25]. Release of the peptides from E5-325 was much less than from T80A (Fig 2B) and the relationship with size was less significant ($R^2 = 0.581$).

The rate of drug release from polymeric matrices has been positively correlated with the rate of hydration [34, 35]. For T80A and E5-325, water uptake over 24 hr was 4.3 ± 0.2 and 2.1 ± 0.1% of the weight of the film, respectively. This difference is in keeping with the faster efflux of the peptides from T80A compared to E5-325 (Fig 2).

3.2 Release of peptides from T80A: effect of media composition.

Due to the relatively low release of each peptide from E5-325, T80A was chosen for further characterization using the cyclic peptide PMX53 and the linear peptide JPE1375. The efflux of PMX53 (Fig 3A) and JPE1375 (Fig 3B) was studied in water, phosphate buffered saline (PBS) and 10% fetal bovine serum in cell culture medium (FBS + RPMI 1640). For PMX53, there was a significant increase in the initial release (burst effect) when incubated in PBS. This was further enhanced in FBS + RPMI 1640. However, after 4 hr, the rate of release was linear and independent of the media used.

For JPE1375, a different release profile was observed. Firstly, efflux was essential first-order with little evidence of a burst effect. Secondly, while PBS enhanced JPE1375 release, FBS + RPMI 1640 did not. Indeed, after 24 hr, there was a significant decrease in the drug concentration in the medium (Fig 3B). This was due to instability of the peptide in the serum, and highlights an advantage of cyclized peptides that are less prone to protease-mediated degradation.

3.3 Release of PMX53 from blended TPUs

Following the observation that peptide release from different TPUs was markedly different, efflux from films generated by mixing T80A with E5-325 was investigated. Because of incompatibility of the hydrophilic hard and hydrophobic soft segments, the blended TPUs generate different micro-domains compared to the individual TPUs. It was reasoned that these different micro-domains may affect drug efflux by influencing the distribution of PMX53, the degree of peptide-polymer interaction or the rate of hydration of

the matrix. For these experiments, PMX53 efflux was determined in FBS-RPMI 1640. Fig 4A shows the progressive decrease in peptide efflux as the percent E5-325 increased. This was primarily due to an inhibition of the burst effect over the first 4 hr of drug release (Fig 4B). After 4 hr, efflux was essentially linear regardless of the TPU mixture used. When PMX53 efflux from the 50:50 blend of the two TPUs was examined over 21 days, release remained linear over the entire time period (Fig. 4C). Release of PMX53 from E5-325 over the same time period was minimal.

3.4 Bioactivity of PMX53 released from T80A

To determine whether PMX53 released from the TPUs was biologically active, the ability of the peptide following efflux from T80A to inhibit C5a-mediated Ca^{2+} mobilization in U937 cells was determined. Fig. 5 shows that 0.1 and 1 μM PMX53 inhibited C5a-mediated Ca^{2+} mobilization by 30% and 99%, respectively. This is consistent with the known potency of PMX53 against the C5a receptor [36]. The drug in the medium after 72 hr was approximately 0.6 μM (Fig 3A) and this inhibited C5a by 89% indicating the PMX53 retained its biological activity during casting of the films and following release.

3.5 In vivo pharmacokinetics of PMX53 released from TPUs

PMX53 administered intraperitoneally was rapidly absorbed and eliminated with a half-life less than 20 min (Fig 6A). This is similar to the reported elimination of the drug in rats [37, 38]. When T80A films loaded with 200 μg of PMX53 were implanted in the peritoneal cavity, the time to peak plasma concentration was extended to 2.5 hr after which plasma levels decreased to less than 10 ng/ml by 24 hr (Fig 6B). The results shown in Fig 6B were

further analyzed by fitting a one-compartment model with first-order absorption and elimination to the data:

$$C = \frac{Dose \cdot k_a}{V_d \cdot (k_a - k_e)} (e^{-k_e t} - e^{-k_a t}) \quad (1)$$

where C is the concentration of PMX53 in plasma at time t, V_d is the volume of distribution, k_a is the absorption rate constant and k_e is the elimination rate constant. The pharmacokinetic parameters for the efflux of PMX53 from T80A are shown in Table 2 and the goodness of fit is shown in Fig 6B (solid line). The volume of distribution (412 ml) indicated that PMX53 distributes extensively into peripheral tissues, which may account, in part, for the very short plasma half-life of the drug *in vivo*.

When PMX53 (200 μg) was administered in a 50% blend of T80A and E5-325, the time to peak plasma concentration was similar to that seen with T80A implants, although the maximum concentration was less (Fig 6C). This resulted from the slower rate of efflux from the implanted polymer disc, as shown in Fig 6D. At 24 hr, the plasma concentration was approximately 40 ng/ml, which slowly decreased to 20 ng/ml by day 9 (Fig 6C). The release of drug from the films recovered at sacrifice showed an initial burst effect (Fig 6D) followed by linear release up to 9 days (Fig 6E).

Equation 2 was fitted to the data of PMX53 released from the blended TPUs. The model comprised a single compartment with first-order absorption and elimination along with an infusion component, which represented the constant release of PMX53 from the polymer after the initial burst effect:

$$C = \frac{Dose \cdot k_a}{V_1 \cdot (k_a - k_e)} (e^{-k_e t} - e^{-k_a t}) + \frac{k_0}{V_2 \cdot k_e} (1 - e^{-k_e (t - T_d)}) \quad (2)$$

where k_0 is infusion rate, determined by the slow rate of efflux from 50% T80A after lag time. T_d is the lag time. For 50% T80A, k_e was assumed to be equal to the k_e determined in modeling release from T80A as it is independent of the TPU used. V_1 is the volume of distribution in the first rapid release process while V_2 is the volume of distribution during the infusion process. The resulting kinetic parameters are shown in Table 2.

The initial burst effect, measured over the first 4 hr, accounted for approximately 25% of the total drug released from the implant (Fig 6E). The area under the concentration-time profile (AUC) was 6 fold greater for the blended TPUs compared to T80A alone. This is consistent with the larger amount of drug released from the blended TPUs (Fig 4D & E). The predicted infusion rate was 615 ng/hr (Table 2), which is similar to the efflux rate of PMX53 from the implant *in vivo* (576 ng/hr – Fig 6E, dotted line).

The model predicted that the volume of distribution was large at early time points, similar to that seen with the T80A implants. At later time points, the volume of distribution decreased to only 33 ml. Time-dependent changes in the apparent volume of distribution is indicative of target-mediated drug disposition[39].

3.6 In vivo bioactivity of PMX53 released from blended TPUs

To determine whether the sustained release of PMX53 *in vivo* could lead to a significant biological effect, the growth of B16-F10 melanoma cells in C57 black mice was investigated. Fig 7A shows the change in body weights for animals implanted with a blended TPU (50% T80A, 50% E5-325) with and without PMX53. There were no differences between the two groups indicating no overt toxicity due to the drug. Fig 7B shows a significant delay in tumor growth in mice implanted with PMX53 compared to controls (2-way ANOVA, $p < 0.01$). Survival curves (Fig 7C) also showed a significant increase in survival for mice implanted

with films containing PMX53 (Chi Squared, $P < 0.01$). These results demonstrated that PMX53 released from implanted TPUs exerts a biological effect, impairs tumor growth and prolongs the survival time in the B16-F10 melanoma model.

4. Discussion

There has been a growing interest in the development of therapeutic peptides because of their specificity and potency [1]. However, peptides have poor bioavailability and very short circulation times *in vivo*, often limiting their clinical use. The current study has shown that biocompatible TPU implants may be a simple and effective means for controlling peptide delivery *in vivo*. These polymers have been widely used in medicine and can be manufactured using a variety of hard and soft segments. Polyurethanes are used to manufacture stents, catheters, pacemaker leads, heart valves, and as components of implantable devices such as artificial joints, spine stabilization devices and disc repacements [40, 41]. Impregnating these polymer components with therapeutics to minimize infections, clotting or inflammatory responses has been reported [19-21], although peptide release has not been extensively investigated.

Drug loading into polymer matrices can be achieved by a variety of different approaches [42-44]. Here, co-casting of the polyurethane in a solvent compatible with the peptides resulted in high loading with no detectable degradation. This method was not only simple but also maximized the amount of drug in the polyurethane, an important outcome for expensive material such as peptides. Two commonly used medical-grade TPUs were studied: Tecoflex 80A (T80A) and Elast-Eon E5-325. Both are aliphatic polyether polyurethanes with different hard and soft segments. The arrangement of these segments creates different compartments within the polymer matrix [25]. Peptide release kinetics from both TPUs

correlated with peptide size and the rate of polymer hydration. The efflux of small molecule drugs from TPUs is also influenced by the osmotic effects of different solutes. This is particularly evident with polymeric hydrogels [45]. As water diffuses into TPU films, it has at least 2 effects. Firstly, it solubilizes the crystalline drug embedded in the film allowing it to diffuse out of the polymer. Secondly, it hydrates the polymer backbone and induces swelling, which is primarily dependent on the soft segment composition [46]. Hydration initially occurs very rapidly followed by an exponential decrease in water uptake, may explain the greater burst effect observed with the T80A polymer compared to E5-325. In sustained drug release models, a burst effect can be advantageous as it rapidly increases the target drug concentration at early time points, similar to a loading dose given before a constant drug infusion.

Previous work has demonstrated that tumour growth is enhanced by an inflammatory environment [47], and that anti-inflammatory drugs decrease the risk of certain cancers such as gastric, colon and breast [48, 49]. PMX53 has been shown to affect ovarian cancer proliferation by inhibiting neovascularization [50] and to inhibit TC-1 tumor formation in a mouse model [51], albeit only following multiple dosing regimens. In addition, PMX53 inhibited the proliferation of B16-F10 melanomas in a syngeneic animal model [52]. In the present study, the effect of TPU-impregnated PMX53 on B16-F10 melanoma growth was assessed. PMX53 plasma levels remained elevated for at least 9 days when implanted in a 50:50 mixture of T80A and E5-325A. Moreover, a significant decrease in tumor proliferation and survival was seen. These data show that peptide release from the TPU matrix was not only sustained but the peptide remained pharmacologically active *in vivo*.

This is the first study to demonstrate that the release of a drug from TPUs can be modified by blending the different polymers. Indeed, different mixtures resulted in different burst effects and rates of drug release. In practice, blending TPUs can be tailored not only for

peptide with different physical properties, but also for other drugs to fine-tune their release kinetics. This study provides important findings for TPU-based therapeutic peptide delivery that could improve the pharmacological utility of peptides as therapeutics.

Acknowledgements

This study was supported by the National Health and Medical Research Council of Australia (Grant #569694). RC is funded by the ARC Future Fellowship scheme.

Reference

[1] Craik DJ, Fairlie DP, Liras S, Price D. The future of peptide-based drugs. Chemical biology & drug design. 2013;81:136-47.

[2] Bellmann-Sickert K, Beck-Sickinger AG. Peptide drugs to target G protein-coupled receptors. Trends in pharmacological sciences. 2010;31:434-41.

[3] Albericio F, Kruger HG. Therapeutic peptides. Future medicinal chemistry. 2012;4:1527-31.

[4] Pereira IHL, Ayres E, Patrício PS, Góes AM, Gomide VS, Junior EP, et al. Photopolymerizable and injectable polyurethanes for biomedical applications: Synthesis and biocompatibility. Acta biomaterialia. 2010;6:3056-66.

[5] Bergmeister H, Seyidova N, Schreiber C, Strobl M, Grasl C, Walter I, et al. Biodegradable, thermoplastic polyurethane grafts for small diameter vascular replacements. Acta biomaterialia. 2015;11:104-13.

[6] Crisante F, Francolini I, Bellusci M, Martinelli A, D'Ilario L, Piozzi A. Antibiotic delivery polyurethanes containing albumin and polyallylamine nanoparticles. European Journal of Pharmaceutical Sciences. 2009;36:555-64.

[7] Da Silva GR, Ayres E, Orefice RL, Moura SAL, Cara DC, Cunha JADS. Controlled release of dexamethasone acetate from biodegradable and biocompatible polyurethane and polyurethane nanocomposite. Journal of drug targeting. 2009;17:374-.

[8] Chen Y, Wang R, Zhou J, Fan H, Shi B. On-demand drug delivery from temperature-responsive polyurethane membrane. Reactive and Functional Polymers. 2011;71:525-35.

[9] Mishra A, Singh SK, Dash D, Aswal VK, Maiti B, Misra M, et al. Self-assembled aliphatic chain extended polyurethane nanobiohybrids: Emerging hemocompatible biomaterials for sustained drug delivery. Acta biomaterialia. 2014;10:2133-46.

[10] Cheng J, Tang X, Zhao J, Shi T, Zhao P, Lin C. Multifunctional cationic polyurethanes designed for non-viral cancer gene therapy. Acta biomaterialia. 2016;30:155-67.

[11] Hernandez R, Weksler J, Padsalgikar A, Runt J. Microstructural organization of three-phase polydimethylsiloxane-based segmented polyurethanes. MACROMOLECULES. 2007;40:5441-9.

[12] Delebecq E, Pascault JP, Boutevin B, Ganachaud F. On the versatility of urethane/urea bonds: reversibility, blocked isocyanate, and non-isocyanate polyurethane. Chemical reviews. 2013;113:80-118.

[13] Nelson DM, Baraniak PR, Ma Z, Guan J, Mason NS, Wagner WR. Controlled release of IGF-1 and HGF from a biodegradable polyurethane scaffold. Pharmaceutical research. 2011;28:1282-93.

[14] Kim J, Hollinger JO. Recombinant human bone morphogenetic protein-2 released from polyurethane-based scaffolds promotes early osteogenic differentiation of human mesenchymal stem cells. Biomedical materials. 2012;7:045008.

[15] Li B, Yoshii T, Hafeman AE, Nyman JS, Wenke JC, Guelcher SA. The effects of rhBMP-2 released from biodegradable polyurethane/microsphere composite scaffolds on new bone formation in rat femora. Biomaterials. 2009;30:6768-79.

[16] Li B, Davidson JM, Guelcher SA. The effect of the local delivery of platelet-derived growth factor from reactive two-component polyurethane scaffolds on the healing in rat skin excisional wounds. Biomaterials. 2009;30:3486-94.

[17] Li X, Wang Y, Chen J, Wang Y, Ma J, Wu G. Controlled release of protein from biodegradable multi-sensitive injectable poly(ether-urethane) hydrogel. ACS applied materials & interfaces. 2014;6:3640-7.

[18] Wang J, Liu Q, Tian Y, Jian Z, Li H, Wang K. Biodegradable hydrophilic polyurethane PEGU25 loading antimicrobial peptide Bmap-28: a sustained-release membrane able to inhibit bacterial biofilm formation in vitro. Scientific reports. 2015;5:8634.

[19] McCann M, Moore ZE. Interventions for preventing infectious complications in haemodialysis patients with central venous catheters. The Cochrane database of systematic reviews. 2010:Cd006894.

[20] Pinto FC, Da Silva-Cunha Junior A, Orefice RL, Ayres E, Andrade SP, Lima LD, et al. Controlled release of triamcinolone acetonide from polyurethane implantable devices: application for inhibition of inflammatory-angiogenesis. Journal of materials science Materials in medicine. 2012;23:1431-45.

[21] Vallejo-Heligon SG, Klitzman B, Reichert WM. Characterization of porous, dexamethasone-releasing polyurethane coatings for glucose sensors. Acta biomaterialia. 2014;10:4629-38.

[22] Wong AK, Finch AM, Pierens GK, Craik DJ, Taylor SM, Fairlie DP. Small molecular probes for G-protein-coupled C5a receptors: conformationally constrained antagonists derived from the C terminus of the human plasma protein C5a. Journal of medicinal chemistry. 1998;41:3417-25.

[23] Chan LY, Gunasekera S, Henriques ST, Worth NF, Le SJ, Clark RJ, et al. Engineering pro-angiogenic peptides using stable, disulfide-rich cyclic scaffolds. Blood. 2011;118:6709-17.

[24] Grishin AA, Cuny H, Hung A, Clark RJ, Brust A, Akondi K, et al. Identifying key amino acid residues that affect alpha-conotoxin AuIB inhibition of alpha3beta4 nicotinic acetylcholine receptors. The Journal of biological chemistry. 2013;288:34428-42.

[25] Zhang J, Martin DJ, Taran E, Thurecht KJ, Minchin RF. Effect of Supercritical Carbon Dioxide on the Loading and Release of Model Drugs from Polyurethane Films: Comparison with Solvent Casting. Macromolecular Chemistry and Physics. 2014;215:54-64.

[26] Solis-Correa RE, Vargas-Coronado R, Aguilar-Vega M, Cauich-Rodriguez JV, Roman JS, Marcos A. Synthesis of HMDI-based segmented polyurethanes and their use in the manufacture of

elastomeric composites for cardiovascular applications. Journal of biomaterials science Polymer edition. 2007;18:561-78.

[27] Detta N, Errico C, Dinucci D, Puppi D, Clarke DA, Reilly GC, et al. Novel electrospun polyurethane/gelatin composite meshes for vascular grafts. Journal of materials science Materials in medicine. 2010;21:1761-9.

[28] Christman MS, L'Esperance JO, Choe CH, Stroup SP, Auge BK. Analysis of ureteric stent kinking forces: the role of curvature in stent failure. BJU international. 2010;105:866-9; discussion 8-9.

[29] Shepherd DE, Johnstone A. A new design concept for wrist arthroplasty. Proceedings of the Institution of Mechanical Engineers Part H, Journal of engineering in medicine. 2005;219:43-52.

[30] Bernacca GM, Straub I, Wheatley DJ. Mechanical and morphological study of biostable polyurethane heart valve leaflets explanted from sheep. Journal of biomedical materials research. 2002;61:138-45.

[31] Handa H, Major TC, Brisbois EJ, Amoako KA, Meyerhoff ME, Bartlett RH. Hemocompatibility Comparison of Biomedical Grade Polymers Using Rabbit Thrombogenicity Model for Preparing Nonthrombogenic Nitric Oxide Releasing Surfaces. Journal of materials chemistry B, Materials for biology and medicine. 2014;2:1059-67.

[32] Proctor LM, Woodruff TM, Sharma P, Shiels IA, Taylor SM. Transdermal pharmacology of small molecule cyclic C5a antagonists. Advances in experimental medicine and biology. 2006;586:329-45.

[33] Schnatbaum K, Locardi E, Scharn D, Richter U, Hawlisch H, Knolle J, et al. Peptidomimetic C5a receptor antagonists with hydrophobic substitutions at the C-terminus: increased receptor specificity and in vivo activity. Bioorg Med Chem Lett. 2006;16:5088-92.

[34] Fu Y, Kao WJ. Drug release kinetics and transport mechanisms of non-degradable and degradable polymeric delivery systems. Expert opinion on drug delivery. 2010;7:429-44.

[35] Gurselt I, Yagmurlu F, Korkusuz F, Hasirci V. In vitro antibiotic release from poly(3-hydroxybutyrate-co-3-hydroxyvalerate) rods. Journal of microencapsulation. 2002;19:153-64.

[36] Woodruff TM, Nandakumar KS, Tedesco F. Inhibiting the C5-C5a receptor axis. Molecular immunology. 2011;48:1631-42.

[37] Morgan M, Bulmer AC, Woodruff TM, Proctor LM, Williams HM, Stocks SZ, et al. Pharmacokinetics of a C5a receptor antagonist in the rat after different sites of enteral administration. Eur J Pharm Sci. 2008;33:390-8.

[38] Strachan AJ, Shiels IA, Reid RC, Fairlie DP, Taylor SM. Inhibition of immune-complex mediated dermal inflammation in rats following either oral or topical administration of a small molecule C5a receptor antagonist. Br J Pharmacol. 2001;134:1778-86.

[39] Mager DE. Target-mediated drug disposition and dynamics. Biochemical Pharmacology. 2006;72:1-10.

[40] Bezuidenhout D, Williams DF, Zilla P. Polymeric heart valves for surgical implantation, catheter-based technologies and heart assist devices. Biomaterials. 2015;36:6-25.

[41] St. John KR. The use of polyurethane materials in the surgery of the spine: a review. The Spine Journal. 2014;14:3038-47.

[42] Champeau M, Thomassin JM, Tassaing T, Jerome C. Drug loading of polymer implants by supercritical CO2 assisted impregnation: A review. J Control Release. 2015;209:248-59.

[43] Calejo MT, Sande SA, Nystrom B. Thermoresponsive polymers as gene and drug delivery vectors: architecture and mechanism of action. Expert opinion on drug delivery. 2013;10:1669-86.

[44] Wischke C, Behl M, Lendlein A. Drug-releasing shape-memory polymers - the role of morphology, processing effects, and matrix degradation. Expert opinion on drug delivery. 2013;10:1193-205.

[45] Kim SW, Bae YH, Okano T. Hydrogels: swelling, drug loading, and release. Pharmaceutical research. 1992;9:283-90.

[46] Green RJ, Corneillie S, Davies J, Davies MC, Roberts CJ, Schacht E, et al. Investigation of the hydration kinetics of novel poly(ethylene oxide) containing polyurethanes. Langmuir. 2000;16:2744-50.

[47] Vakkila J, Lotze MT. Inflammation and necrosis promote tumour growth. Nat Rev Immunol. 2004;4:641-8.

[48] Gonzalez-Perez A, Garcia Rodriguez LA, Lopez-Ridaura R. Effects of non-steroidal anti-inflammatory drugs on cancer sites other than the colon and rectum: a meta-analysis. BMC cancer. 2003;3:28.

[49] Wang WH, Huang JQ, Zheng GF, Lam SK, Karlberg J, Wong BC. Non-steroidal anti-inflammatory drug use and the risk of gastric cancer: a systematic review and meta-analysis. Journal of the National Cancer Institute. 2003;95:1784-91.

[50] Nunez-Cruz S, Gimotty PA, Guerra MW, Connolly DC, Wu YQ, DeAngelis RA, et al. Genetic and pharmacologic inhibition of complement impairs endothelial cell function and ablates ovarian cancer neovascularization. Neoplasia. 2012;14:994-1004.

[51] Markiewski MM, DeAngelis RA, Benencia F, Ricklin-Lichtsteiner SK, Koutoulaki A, Gerard C, et al. Modulation of the antitumor immune response by complement. Nat Immunol. 2008;9:1225-35.

[52] Janelle V, Langlois MP, Tarrab E, Lapierre P, Poliquin L, Lamarre A. Transient complement inhibition promotes a tumor-specific immune response through the implication of natural killer cells. Cancer Immunol Res. 2014;2:200-6.

Table 1
The chemical structure of peptides used in the current study.

Name	Mol Wt	Structure	Target
PMX53	895	Ac-Phe-Orn-Pro-Cha-Trp-Arg |_____|	C5α receptor
JPE1375	954	Ho-Phe-Orn-Pro-Hle-Phe-Phe-NH_2	C5α receptor
PMX201	896	Ac-Phe-Orn-Pro-Cha-Trp-Cit |_____|	C5α receptor
PMX205	838	Hyc-Orn-Pro-Cha-Trp-Arg |_____|	C5α receptor
SFT-1	1512	Gly-Arg-Cys-Thr-Lys-Ser-Ile-Pro-Pro-Ile-Cys-Phe-Pro-Asp	Protease
Xen2174	1403	Glu/Gln-Gly-Val-Cys-Cys-Gly-Tyr-Lys-Leu-Cys-His-Orn-Cys	Noradrenalin transporter

Ho = l-hydroorotic acid, Hle = d-homoleucine, Cit = citulline, Cha = cyclohexylalanine, Hyc = hydrocinnamate. All other amino acids are represented by their standard 3 letter codes.

Table 2
Pharmacokinetic parameters for the efflux of PMX53 from T80A and from 50% T80A *in vivo*.

TPU	AUC (ng h/ml)	$t_{1/2}$ (h)	V_d (ml)	k_a (hr^{-1})	k_e (hr-1)	k_0 (ng/hr)	T_d (hr)
T80A	907	0.98	412	0.32	0.7	-	-
50% T80A, 50% E5-325	5441	0.98	V_1 =282 V_2 =33	0.79	0.7	615	0.29

AUC: area under the curve; $t_{1/2}$: half-life; V_d: volume of distribution; k_a: absorption rate constant; k_e: elimination rate constant; k_0: infusion rate; T_d: lag time.

Legends to Figures:

Fig 1. Time dependent release of peptides from T80A. ● PMX205, □ PMX201, o PMX53, ■ JPE1375, ▽ Xen2174, ▲ SFT-1. Each point is the mean ± s.e.m., n = 3.

Fig 2. Effect of size (molecular weight) on the release of peptides from TPUs. A. Relationship between the cumulative release of peptides from T80A over 72 hr and their molecular weights. B. Relationship between the cumulative release of peptides from E5-325 over 72 hr and their molecular weights.

Fig 3. Efflux of C5aR antagonists from T80A in different media. Efflux of PMX53 (A) and JPE1375 (B) from T80A in PBS (□), 10%FBS-RPMI (●) and H_2O (o). All data are mean ± s.e.m, n = 3. * = significantly different to H_2O by ANOVA ($p < 0.001$)

Fig 4. Effect of blending TPUs on the release of PMX53. (A) Efflux of peptide from films comprised of different percentages of each TPU over 3 days in 10% FBS-RPMI 1640. (B) The initial burst effect, measured as release over the first 4 hr, increased as the percent T80A increased. (C) Efflux of PMX53 from 50% T80A and E5-325 over 21 days in 10% FBS-RPMI1640. All results are mean ± s.e.m, n = 3. * = significantly different to T80A by ANOVA ($p < 0.001$)

Fig 5. Bioactivity of PMX53 following efflux from T80A TPU. Differentiated U937 cells were pre-treated with PMX53 or released peptide and then exposed to 10 nM C5a. Calcium mobilisation was quantified and normalised to C5a alone. Data are mean ± s.e.m, n = 3.

Asterisks indicated significant difference compared to C5a alone by 1 way ANOVA (* = $p < 0.01$; ** = $p<0.001$).

Fig 6. PMX53 plasma levels following intraperitoneal administrated. (A) PMX53 plasma levels following administration of 1 mg/kg PMX5. (B) PMX53 plasma levels following implantation of PMX53-loaded (200 µg) T80A into the peritoneal cavity. The solid curve represents the predicted plasma concentrations from equation 1. (C) PMX53 plasma levels following implantation of PMX53-loaded (200 µg) blended TPU (50% T80A 50% E5-325) into the peritoneal cavity. The solid curve represents the predicted plasma concentrations from equation 2. (D) The in vivo efflux of PMX53 from T80A (o) and 50% T80A, 50% E5-325 (●) over 24 h. (E) The in vivo efflux of PMX53 from the blended TPU over 9 days. Dotted line indicates the linear efflux of PMX53 with time. All results are mean ± s.e.m, n =3. Asterisks indicated significant difference compared to T80A by ANOVA ($p < 0.001$)

Fig 7. Effect of PMX53 released from TPUs on B16-F10 melanoma tumor growth. (A) Body weight of mice implanted with 50% T80A films or PMX53-loaded 50% T80A. (B) Tumor growth in mice implanted with 50% T80A/50% E5234 or PMX53-loaded (200 ug) blended TPU. There was a significant difference in tumour growth between the two groups ($p > 0.01$, ANOVA) (C) Survival curves of mice implanted with blank 50% T80A films or PMX53-loaded 50% T80A. All results are mean ± s.e.m, n = 6. Asterisks indicated significant difference compared to TPU alone by ANOVA ($p < 0.001$)

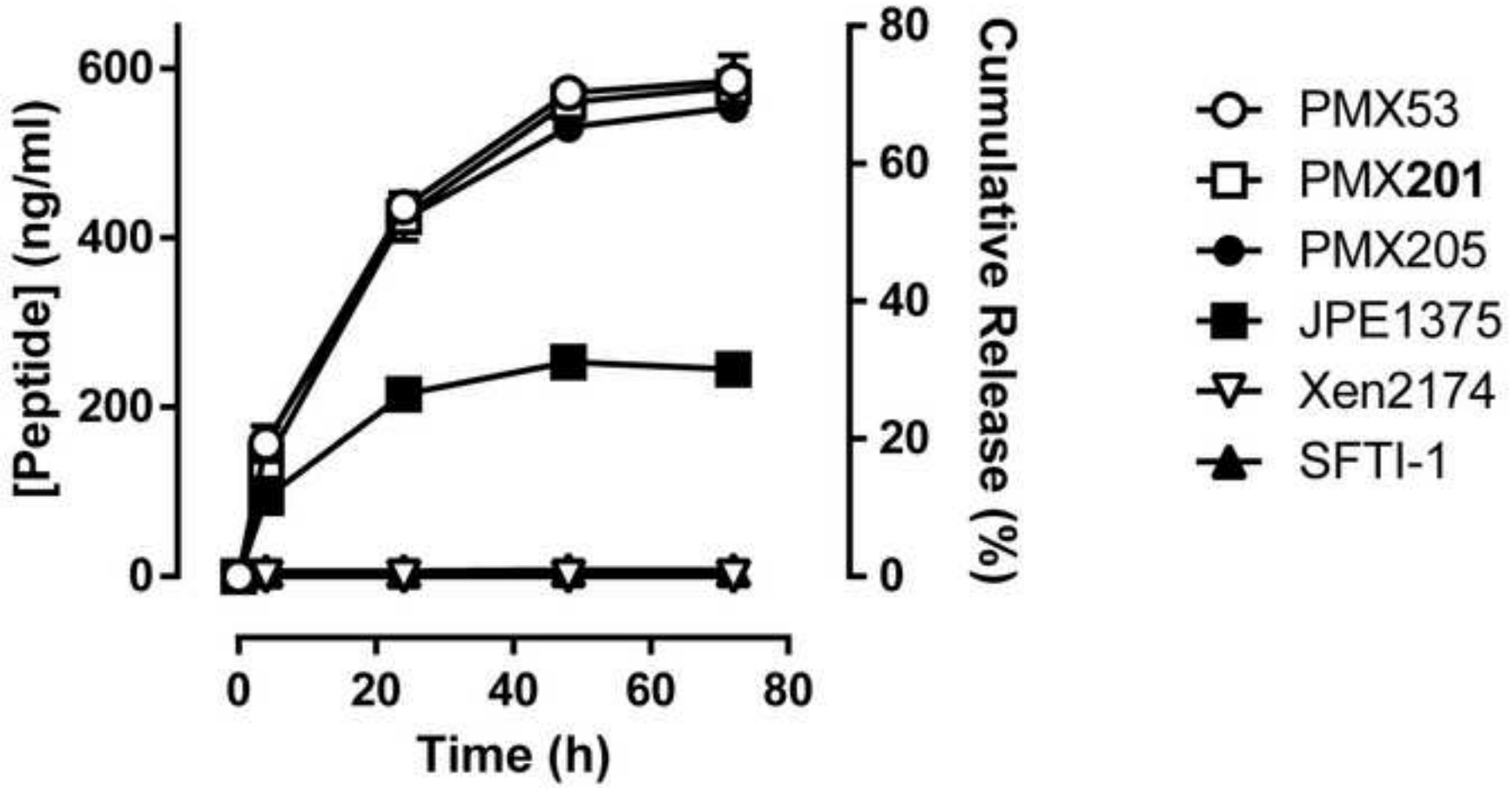

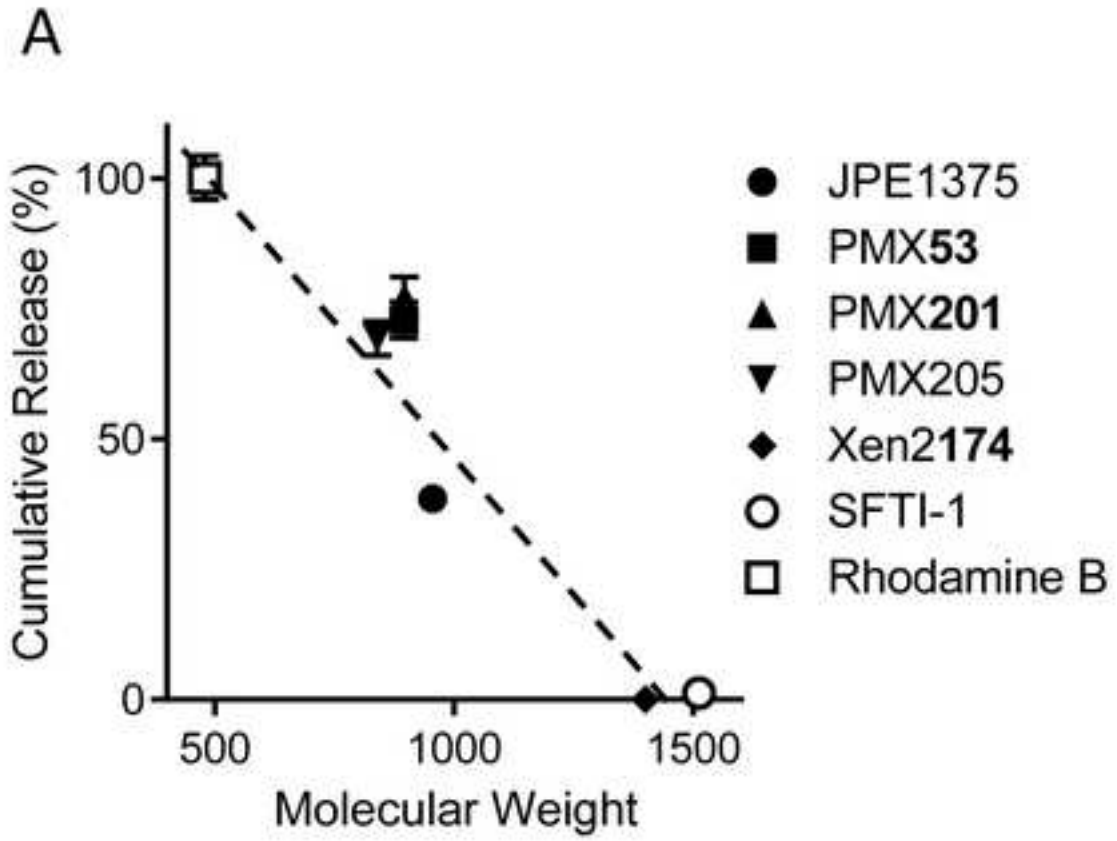
A
Cumulative Release (%)
100
50
0
500
1000
1500
Molecular Weight
JPE1375
PMX53
PMX201
PMX205
Xen2174
SFTI-1
Rhodamine B

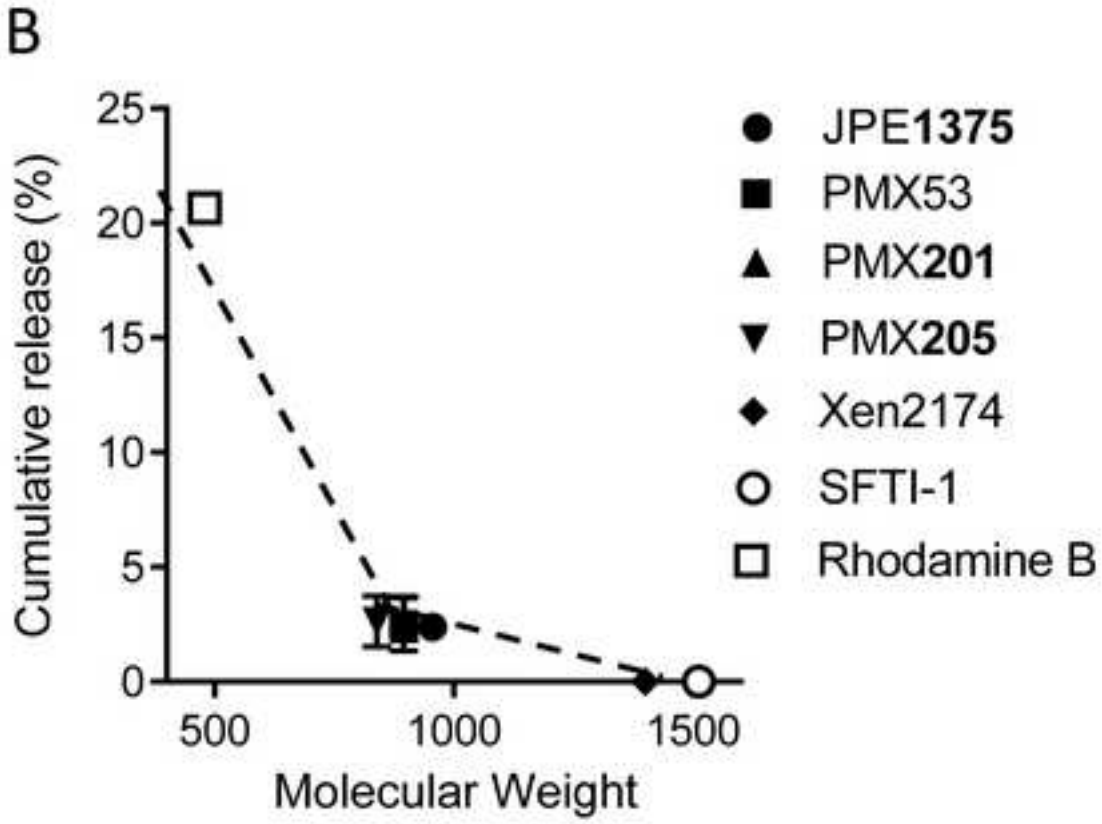
B
Cumulative release (%)
25
20
15
10
5
0
500
1000
1500
Molecular Weight
JPE1375
PMX53
PMX201
PMX205
Xen2174
SFTI-1
Rhodamine B

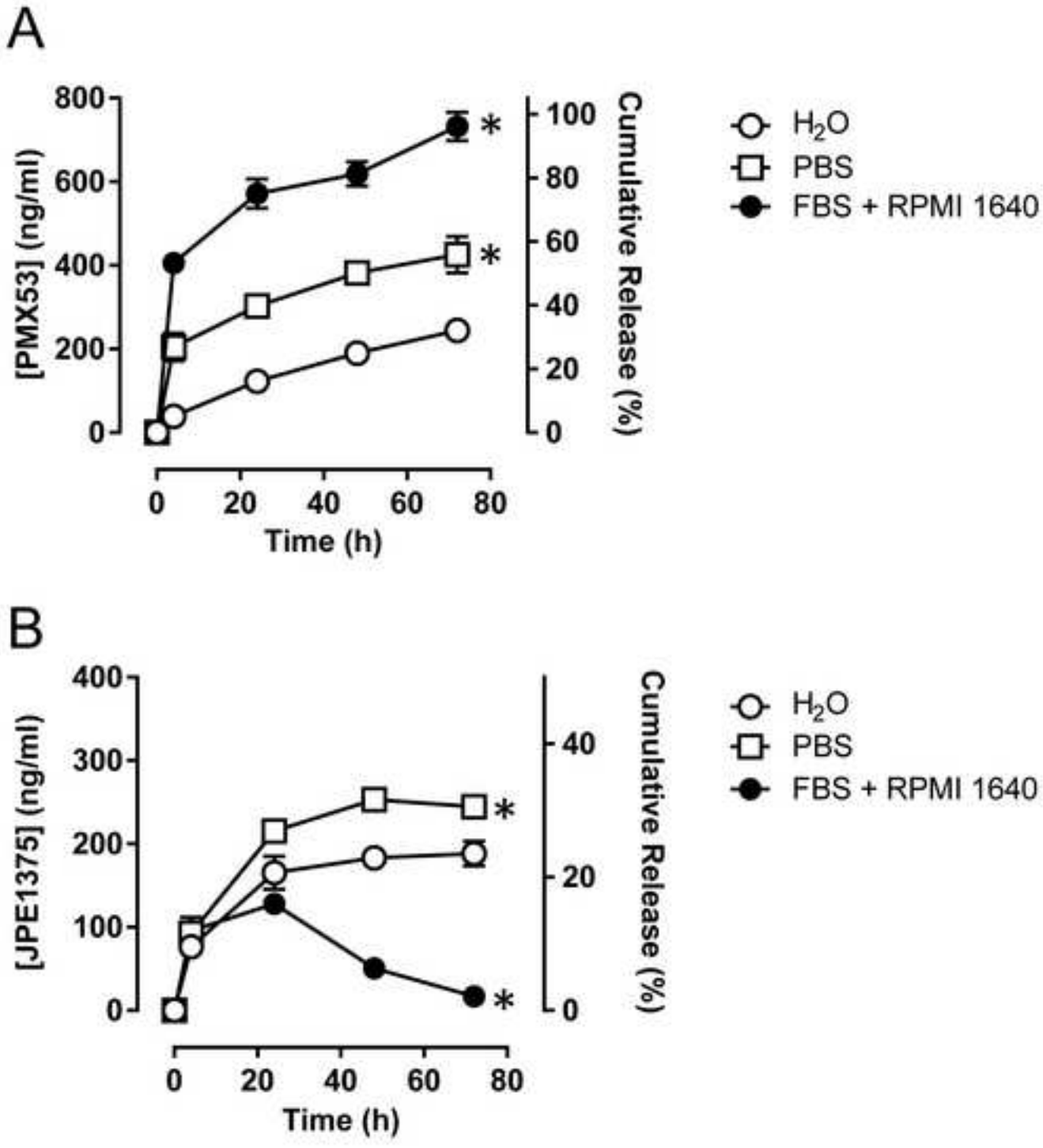
A
[PMX53] (ng/ml)
800
600
400
200
0
100
80
60
40
20
0
Cumulative Release (%)
0
20
40
60
80
Time (h)
*
*
H2O
PBS
FBS + RPMI 1640
B
[JPE1375] (ng/ml)
400
300
200
100
0
40
20
0
Cumulative Release (%)
0
20
40
60
80
Time (h)
*
*
H2O
PBS
FBS + RPMI 1640

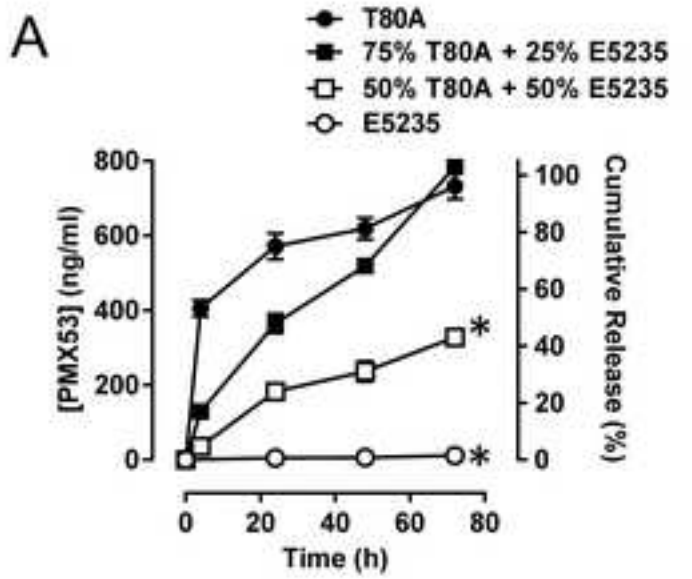

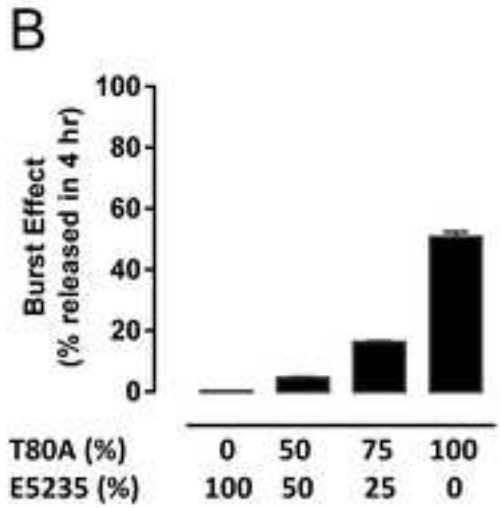

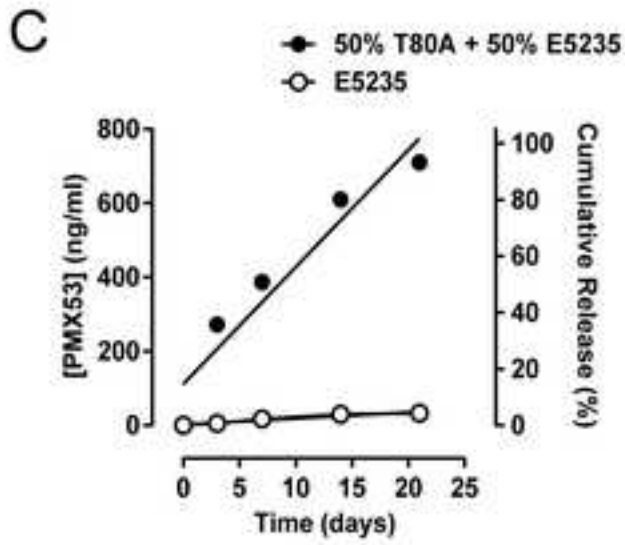

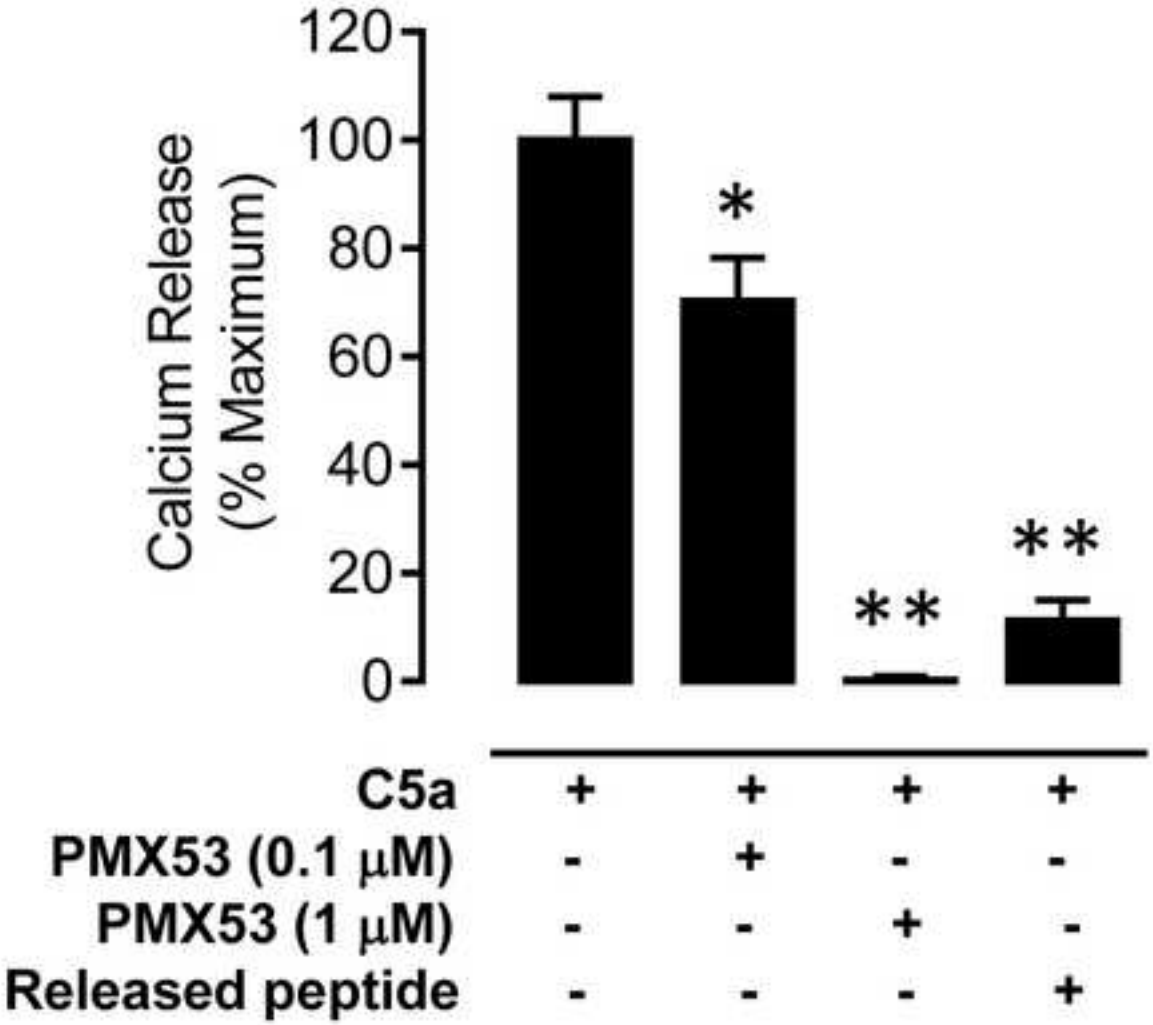
Calcium Release
(% Maximum)
120
100
80
60
40
20
0
*
**
**
C5a + + + +
PMX53 (0.1 μM) - + - -
PMX53 (1 μM) - - + -
Released peptide - - - +

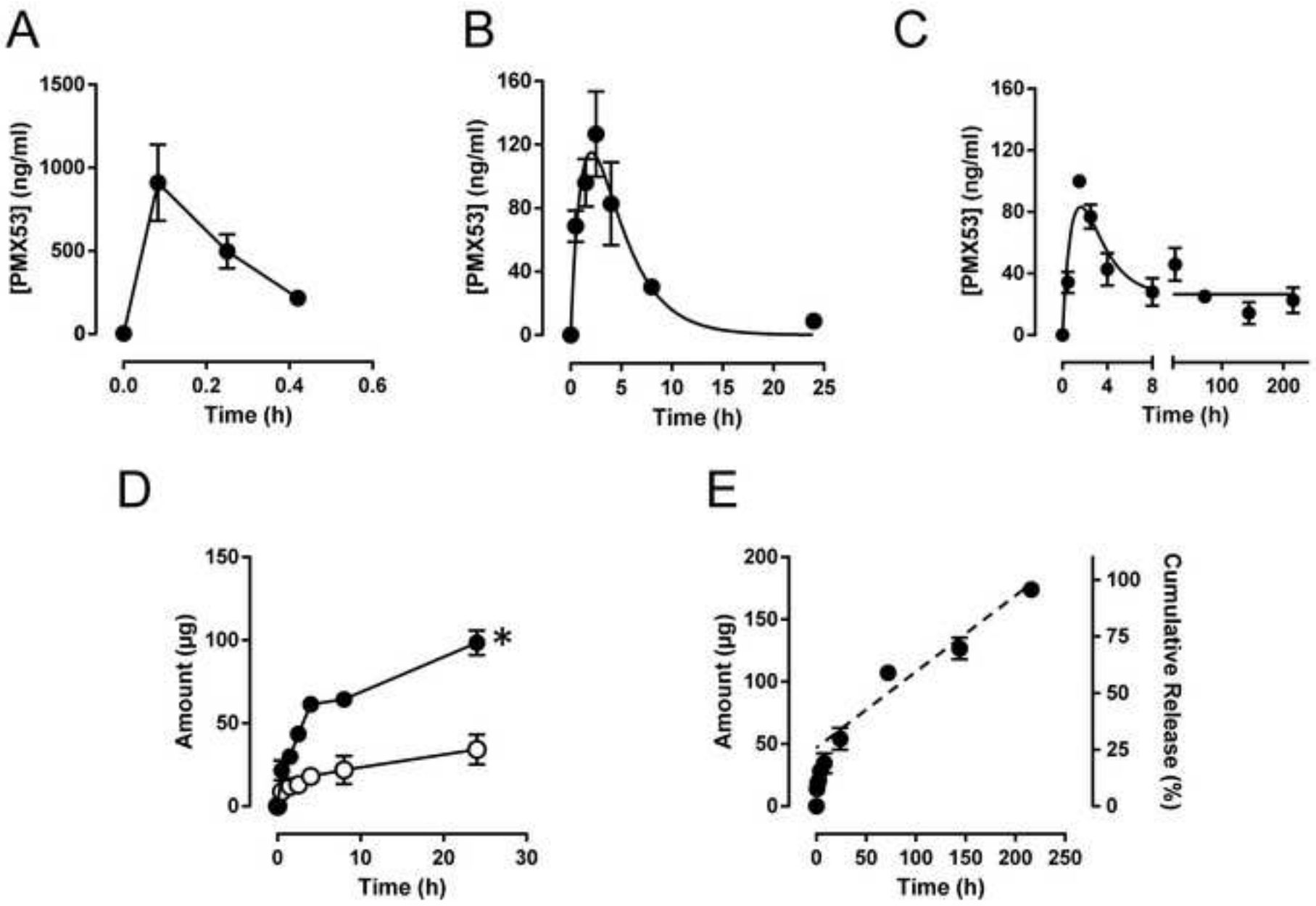

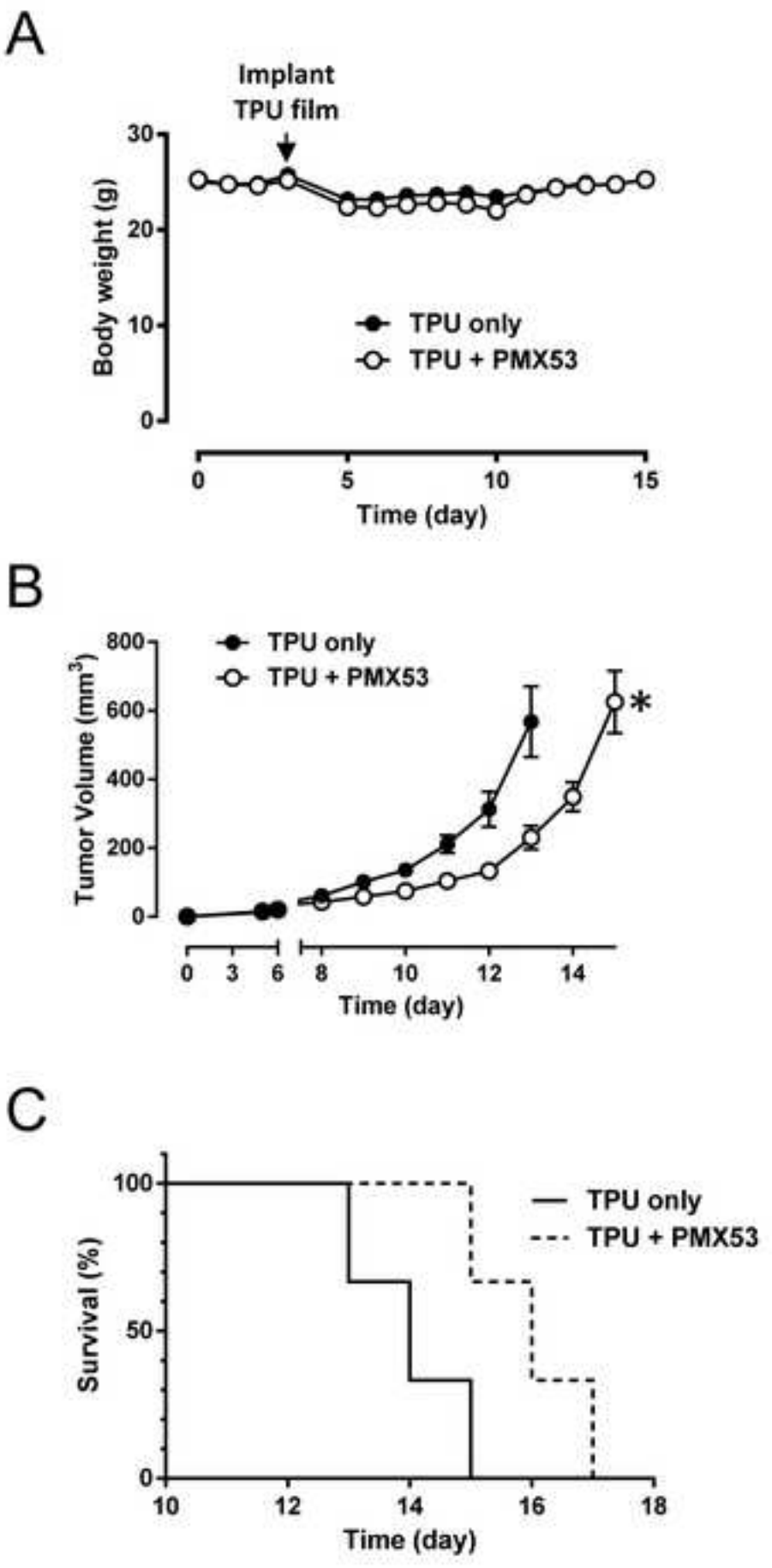

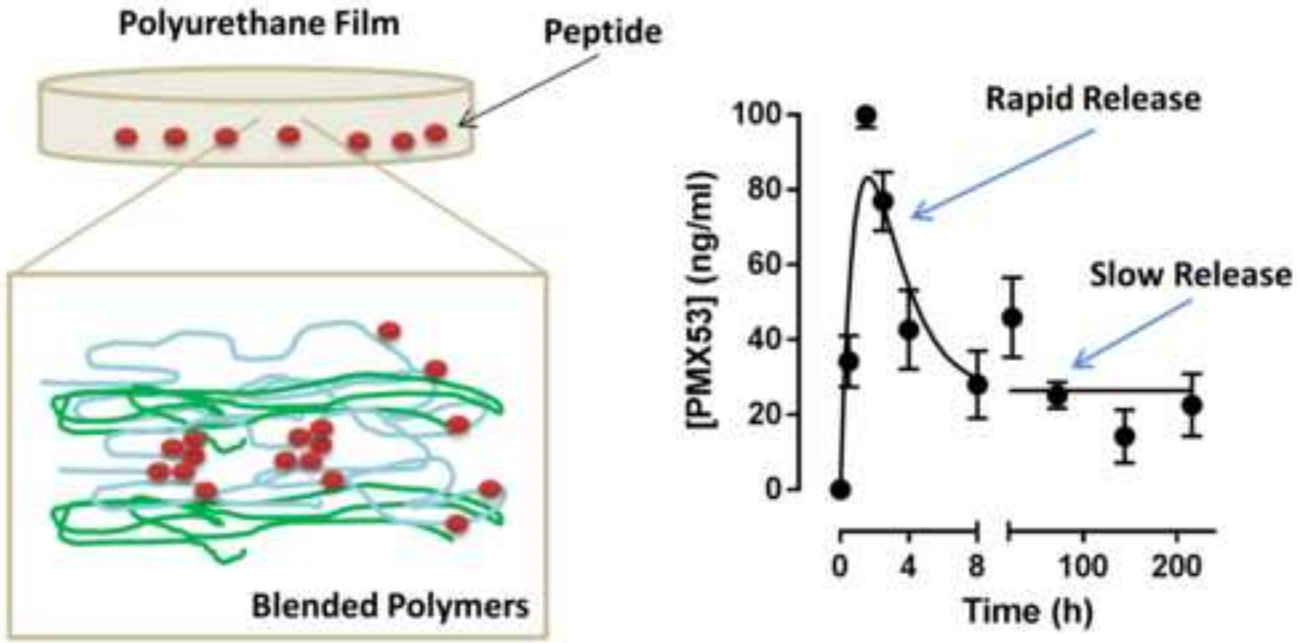

Statement of Significance.

Therapeutic peptides can be highly specific and potent pharmacological agents, but are poorly absorbed and rapidly degraded in the body. This can be overcome by using a matrix that protects the peptide *in vivo* and promotes its slow release so that a therapeutic effect can be achieved over days or weeks. Thermoplastic polyurethanes are a versatile family of polymers that are biocompatible and used for medical implants. Here, the release of several peptides from a range of polyurethanes was shown to depend on the type of polymer used in the polyurethane. This is the first study to examine polyurethane blends for peptide delivery and shows that the rate and extent of peptide release can be fine-tuned using different hard and soft segment mixtures in the polymer.